Technical Notes

TECHNICAL NOTES are short manuscripts describing new developments or important results of a preliminary nature. These Notes cannot exceed 6 manuscript pages and 3 figures; a page of text may be substituted for a figure and vice versa. After informal review by the editors, they may be published within a few months of the date of receipt. Style requirements are the same as for regular contributions (see inside back cover).

New Correlation of Roughness Density Effect on the Turbulent Boundary Layer

Asher Sigal* and James E. Danberg†
U.S. Army Ballistic Research Laboratory, Arberdeen Proving Ground, Maryland 21005

I. Introduction

THE method of equivalent sand roughness is often used in the prediction of turbulent boundary layers over rough surfaces. The method, conceived by Schlichting,[1] relates the effect of actual roughness geometries to that of closely packed sand grains, under the same flow conditions. The well-established data base of Nikuradse[2] is used as the standard and provides the baseline skin-friction relationship.

Schlichting[1] established that the effect of roughness on the law of the wall is a shift of the logarithmic profile. For the fully rough case, the change in the intercept takes the form as indicated in the last term, in brackets, of the following law of the wall:

$$\frac{u}{u_\tau}=\frac{1}{\kappa}\ell n\frac{u_\tau y}{\nu}+C-\left\{\frac{1}{\kappa}\ell n\frac{u_\tau h}{\nu}+D\right\} \tag{1}$$

where D is a function of the geometry, the density, and the arrangement of the roughness elements. For sand roughness, Nikuradse[2] established $D_s=-3.0$. For other roughnesses of height h, the equivalent sand roughness is obtained by equating the wall law intercepts yielding

$$\frac{h_{es}}{h}=\exp[\kappa(3.0+D)] \tag{2}$$

Previous authors have attempted to correlate the term D in Eq. (1) with roughnes density. The objective of the present work is to develop a new correlation, based on a wider and more accurate data base. Emphasis is on the case of two-dimensional roughness, composed of continuous transverse elements.

II. Review of Existing Correlations

A pioneering attempt to quantify the effect of the spacing of two-dimensional roughness elements was performed by Bettermann[3] in 1965. For roughness composed of transverse square bars, he correlated the change of the intercept by the relationship:

$$D=17.55(1.634\log\lambda_h-1.0) \tag{3}$$

where the roughness density parameter is the pitch-to-height ratio, $\lambda_h=p/h$.

In 1969, Dvorak[4] introduced pitch-to-width ratio as a density parameter, $\lambda_a=p/a$. For parameter values less than 5.0, he corroborated Bettermann's correlation. For larger values, the data of Schlichting and others were used to establish a complementary correlation.

In 1973, Simpson[5] suggested a more general interpretation of the Bettermann-Dvorak correlation by taking the reference-area-to-total-frontal area ratio, $\lambda_f=S/S_f$, as a density parameter. The reference area is the area of the smooth surface before adding on the roughness. By examining additional data, he found 1) for low values of the density parameter two branches exist, depending on the formation or absence of transverse vortices between roughness elements, and 2) the shape of the element is important.

A correlation which considered the shape of the elements was reported by Dirling[6] in 1973, in which he included the mean windward surface inclination. His combined roughness density and shape parameter is

$$\Lambda=\frac{d}{h}\left(\frac{A_f}{A_s}\right)^{-(4/3)} \tag{4}$$

where d is the average element spacing, A_s is the windward wetted surface area, and A_f is the frontal area of an element. In 1975, Grabow and White[7] verified Dirling's correlation using new data.

Dalle Donne and Meyer[8] experimented with annuli whose inner surface was roughened by ribs having rectangular cross sections. They correlated their data, and those of 18 previous researchers, using the roughness density parameter:

$$\lambda_h^*=\frac{p-a}{h}=\lambda_h-\frac{a}{h} \tag{5}$$

Their parameter was applied to square and near square rods, where $(0.95\le h/a\le 1.05)$. The Dalle Donne and Meyer[8] parameter is related to that of Bettermann[3] for this case by $\lambda_h^*\approx\lambda_h-1.0$.

III. New Correlation

Since the above correlations were published, additional data have been reported. Furthermore, Coleman et al.[9] re-evaluated Schlichting's experimental data. Their corrected values for the equivalent sand roughness are smaller, and in some cases much smaller, than those reported in Ref. 1 and used in the previous correlations. Coleman et al. re-evaluated three out of four of the groups of roughnesses tested by Schlichting. The fourth group, that of short angles, has been corrected using a correlation of the available corrected vs uncorrected values. The uncertainty involved in this approximation is smaller than the scatter in the data.

A study of the available data, including the corrected data, showed that Simpson's roughness density parameter correlated two- and three-dimensional roughness data best. Also, the inclusion of a shape factor is needed in order to represent data from elements of different shapes. The proposed roughness density parameter is

$$\Lambda_s=\frac{S}{S_f}\left(\frac{A_f}{A_s}\right)^{-1.6} \tag{6}$$

Received April 4, 1988; revision received April 4, 1989.

*NRC Research Associate. Member AIAA.
†Aerospace Engineer. Associate Fellow AIAA.

and the correlation for D is shown in Fig. 1. The sources of the data are summarized in Table 1. Note that the previous correlations, as plotted in Fig. 1, are only valid for square or nearly square bars. The shape factor, in this case, becomes unity so that the former roughness density parameters are all identical to the current one. The exponent of the shape factor in the current parameter was adjusted so that it correlates Schlichting's corrected data for all four groups of elements. In the case of circular rods,[17,18] the streamwise area, below the point of maximum width, was set equal to the frontal area.

The correlation of the three-dimensional data is consistently lower than that of two-dimensional roughnesses. The difference is expected because the end effects of the finite-width elements reduce their form drag relative to continuous transverse ones.

For low values of the roughness density parameter, the Bettermann relationship of Eq. (3) is retained. For moderate and high values of the density parameter, this work proposes for

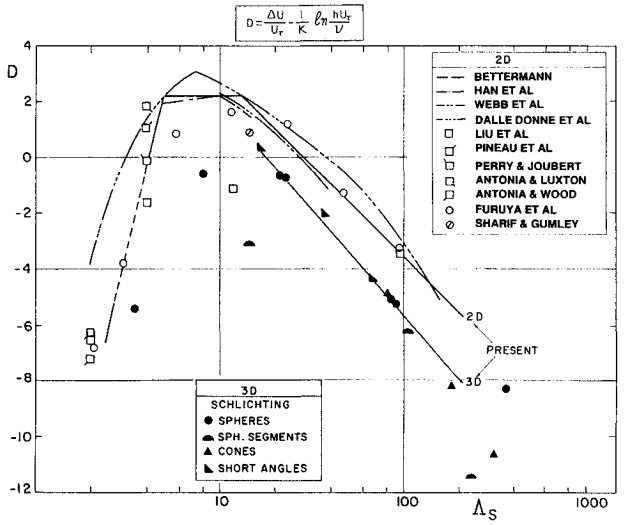

Fig. 1 Correlation of the effect of roughness density on the law of the wall intercept.

Table 1 Sources of data used in the correlation

Authors	λ_h range	Comments
Schlichting[1]	0.9–9.7	Spheres
	2.6–15.3	Spherical segments
	5.3–10.7	Cones
	6.7–13.3	Short angles
Bettermann[3]	2.65–4.18	Low-speed wind tunnel, square bars
Dalle Donne and Meyer[8]	4.08–61.5	Annular tube, rough inner rod. Correlation includes data of several researchers and cover $2.0 \le \lambda_h \le 160.0$
Webb et al.[10]	10.0–40.0	Tubes
Han et al.[11]	5.0–15.0	Parallel plates, only data for transverse ribs used
Liu et al.[12]	2.0–96.0	Water tunnel
Pineau et al.[13]	4.0	Low-speed wind tunnel, square bars
Perry and Joubert[14]	4.0	Low-speed wind tunnel, square bars
Antonia and Luxton[15]	4.0	Low-speed wind tunnel, square bars
Antonia and Wood[16]	2.0	Low-speed wind tunnel, square bars
Furuya et al.[17]	2.0–64.0	Transverse circular rods
Sherif and Gumley[18]	10.0	

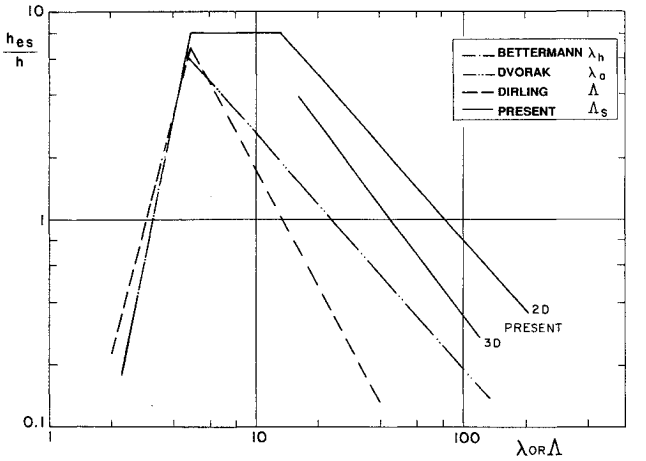

Fig. 2 Correlation of the effect of roughness density on the equivalent sand roughness.

two-dimensional roughness;

$$D=\begin{cases} 17.35(1.634\log\Lambda_s-1.0) & 1.4\le\Lambda_s\le 4.89 \\ 2.2 & 4.89<\Lambda_s<13.25 \\ 9.55(1.0-0.686\log\Lambda_s) & 13.25\le\Lambda_s\le 100.0 \end{cases} \tag{7}$$

For dense arrangements of two-dimensional roughness elements, vortices form in the cavities and the external flow skims over the elements and the vortices. Since no other data on closely packed roughness configurations were found, the left branch of the correlation only should be used for square or nearly square bars.

Using Eq. (2), the equivalent sand roughness for two-dimensional roughness becomes

$$\frac{h_{es}}{h}=\begin{cases} 0.003215\Lambda_s^{4.925} & 1.4\le\Lambda_s\le 4.89 \\ 8.0 & 4.89<\Lambda_s<13.25 \\ 151.71\Lambda_s^{-1.1379} & 13.25\le\Lambda_s\le 100.0 \end{cases} \tag{8}$$

These correlation formulas are plotted in Fig. 2 and compared to the earlier correlations. The present left branch is identical to that of Bettermann and very close to that of Dirling. On the other hand, the right branch is much higher than the previous correlations by Dvorak[4] and Dirling[6] and to a three-dimensional correlation similar to the third element in Eq. (8) and as shown in Fig. 2.

IV. Summary

Based on a review of previous correlations of the effect of roughness on the turbulent boundary layer, a new roughness density parameter is proposed. It is a product of the total-surface-to-total-frontal area ratio and a shape factor which takes into account the average inclination of the windward surface of the roughness elements. The new parameter is used to correlate the displacement of the logarithmic-wall profile for two-dimensional and three-dimensional roughness elements. The equivalent sand roughness of the new correlation is in good agreement with previous ones, for small values of the roughness density parameter. However, for large values of this parameter, the differences are large.

References

[1]Schlichting, H., *Boundary-Layer Theory,* 7th ed., McGraw-Hill Book Company, New York, 1979, pp. 615–626.

[2]Nikuradse, J., "Stromungsgesetze in Rauhen Rohren," *Forschg. Arbeiten Ing.-Wesen,* Vol. 361, July/Aug. 1933.

[3]Bettermann, D., "Contribution a l'Etude de la Convection Force Turbulente le Long de Plaques Rugueuses," *International Journal of Heat and Mass Transfer,* Vol. 9, March 1966, pp. 153-164.

[4]Dvorak, F. A., "Calculation of Turbulent Boundary Layers on Rough Surfaces in Pressure Gradient," *AIAA Journal,* Vol. 7, Sept. 1969, pp. 1752-1759.

[5]Simpson, R. L., "A Generalized Correlation of Roughness Density Effects on the Turbulent Boundary Layer," *AIAA Journal,* Vol. 11, Feb. 1973, pp. 242-244.

[6]Dirling, R. B., Jr., "A Method for Computing Roughwall Heat-Transfer Rates on Re-Entry Nose Tips," AIAA Paper 73-763, July 1973.

[7]Grabow, R. M. and White, C.O., "Surface Roughness Effects on Nose Tip Ablation Characteristics," *AIAA Journal,* Vol. 13, May 1975, pp. 605-609.

[8]Donne, M., and Meyer, L., "Turbulent Convective Heat Transfer from Rough Surfaces with Two-Dimensional Rectangular Ribs," *International Journal of Heat and Mass Transfer,* Vol. 20, June 1977, pp. 583-620.

[9]Coleman, H. W., Hodge, B. K., and Taylor, R. P., "A Reevaluation of Schlichting's Surface Roughness Experiment," *Journal of Fluid Engineering,* Vol. 106, March 1984, pp. 60-65.

[10]Webb, R. L., Eckert, E. R. G., and Goldstein, R. J., "Heat Transfer and Friction in Tubes with Repeated Rib Roughness," *International Journal of Heat and Mass Transfer,* Vol. 14, April 1971, pp. 601-617.

[11]Han, J. C., Glickman, L. R., and Rohsenow, W. M., "An Investigation of Heat Transfer and Friction for Rib-Roughened Surfaces," *International Journal of Heat and Mass Transfer,* Vol. 21, Aug. 1978, pp. 1143-1156.

[12]Liu, C. K., Kline, S. J., and Johnston, J. P., "An Experimental Study of Turbulent Boundary Layer on Rough Walls," Dept. of Mechanical Engineering, Stanford Univ., Rept. MD-15, 1966.

[13]Pineau, F., Nguyen, V. D., Dickinson, J., and Belanger, J., "Study of a Flow Over a Rough Surface with Passive Boundary-Layer Manipulators and Direct Wall Drag Measurements," AIAA Paper 87-0357, 1987.

[14]Perry, A. E., and Joubet, P. N., "Rough-Wall Boundary Layers in Adverse Pressure Gradients," *Journal of Fluid Mechanics,* Vol. 17, Pt. 2, Oct. 1963, pp. 193-211.

[15]Antonio, R. A. and Luxton, R. E., "The Response of a Turbulent Boundary Layer to a Step Change in Surface Roughness, Pt. 1. Smooth to Rough," *Journal of Fluid Mechanics,* Vol. 48, Pt. 4, Aug. 1971, pp. 721-762.

[16]Antonia, R. A., and Wood, D. H., "Calculation of a Turbulent Boundary Layer Downstream of a Step Change in Surface Roughness," *Aeronautical Quarterly,* Vol. 26, Pt. 3, Aug. 1975, pp. 202-210.

[17]Furuya, Y., Fujita, H., and Nakashima, H., "Turbulent Boundary Layers on Plates Roughened by Wires in Equal Intervals," Data Reported by I. Tani in *Perspectives in Turbulence Studies,* Springer-Verlag, Berlin, West Germany, 1987, pp. 223-249.

[18]Sherif, N., and Gumley, P., "Heat-Transfer and Friction Properties of Surfaces with Discrete Roughnesses," *International Journal of Heat and Mass Transfer,* Vol. 9, Dec. 1966, pp. 1297-1320.

Analysis of Transonic Integral Equations: Part II—Boundary Element Methods

W. Ogana*
University of Nairobi, Nairobi, Kenya

Introduction

THE transonic integro-differential and integral equations have normally been solved by constant elements, except in the case of Nixon[1] who solved the equation involving a decay function by using a linear interpolation function to express the transverse variation of the streamwise velocity in each horizontal strip in terms of values on the strip edges. Research in boundary element methods has revealed that constant elements are the simplest of a class of methods and that better accuracy may be achieved by using higher-order elements.[2] In this paper we formulate the boundary element solutions of the two-dimensional transonic integro-differential and integral equations as developed in Part I.[3] Apart from using constant and quadrilateral elements, we develop hybrid elements based on constant elements in the streamwise direction and variable elements in the transverse direction. This leads to constant-linear and constant-quadratic elements. The boundary conditions term is computed using linear and quadratic elements, in addition to constant elements. Computation is carried out for nonlifting parabolic-arc and NACA0012 airfoils.

Received March 27, 1987; revision received Nov. 21, 1988.

*Associate Professor, Department of Mathematics. Member AIAA.

Boundary Element Methods

The basic equations to be solved are Eqs. (5) and (8) of Part I. The computational domain is discretized into surface elements of suitable shapes. We use rectangular elements, with m elements in each of the n horizontal strips. Hence there are $M=mn$ elements denoted $\Delta_1,\Delta_2,\ldots,\Delta_M$, starting from the bottom left and proceeding from left to right in each horizontal strip. Let Δ_j have width $2\delta_j$, height $2h_j$, aspect ratio $\alpha_j=h_j/\delta_j$, and center with coordinates (X_j,Y_j). Solutions are obtained at the N nodes labeled $Q_1,Q_2,\ldots,Q_N$, starting from the bottom left and proceeding from left to right in each row. Let Q_i have coordinates (x_i,y_i).

Uniform treatment can be given to the numerical solution of the integro-differential and integral equations, as shown in Part I. Application of these equations at Q_i yields the nonlinear system

$$\psi_i=\psi_i^B+\sum_{j=1}^{M} I_j, \qquad i=1,2,\ldots,N \tag{1}$$

where

$$I_j=\int_{\Delta_j}\int K(\xi-x_i,\zeta-y_i)H(\xi,\zeta)\,dS \tag{2}$$

while ψ_i,ψ_i^B, K, and H are defined in Part I. The various boundary element methods depend on how Eq. (2) is approximated.

Constant Elements

We assume that H is constant within Δ_j and takes the value at the node Q_j, appropriately located in Δ_j such that $x_j=X_j$. If Δ_j touches the x axis, the node is located on the x axis, marked o and labeled 1 in Fig. 1. Otherwise, the node is located at the center of Δ_j, marked o and labeled 3 in Fig. 1. There is one

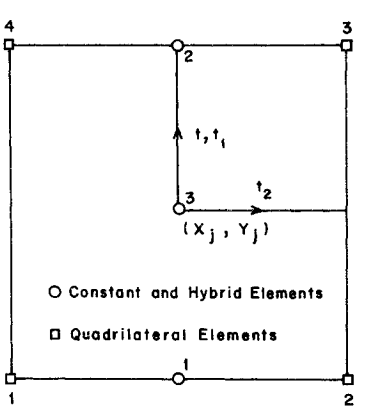

Fig. 1 Location and numbering of nodes within the rectangular element.